NASA TM X-253

NASA TM X-253

TECHNICAL MEMORANDUM

X-253

EXPERIMENTS WITH HYDROGEN AND OXYGEN IN REGENERATIVE ENGINES AT CHAMBER PRESSURES FROM 100 TO 300 POUNDS PER SQUARE INCH ABSOLUTE

By William A. Tomazic, Edward R. Bartoo, and R. James Rollbuhler

Lewis Research Center
Cleveland, Ohio

NATIONAL AERONAUTICS AND SPACE ADMINISTRATION
WASHINGTON
April 1960

NATIONAL AERONAUTICS AND SPACE ADMINISTRATION

TECHNICAL MEMORANDUM X-253

EXPERIMENTS WITH HYDROGEN AND OXYGEN IN REGENERATIVE ENGINES AT CHAMBER PRESSURES FROM 100 TO 300 POUNDS PER SQUARE INCH ABSOLUTE*

By William A. Tomazic, Edward R. Bartoo
and R. James Rollbuhler

SUMMARY

Tests were made with hydrogen and oxygen in regenerative thrust chambers of lightweight construction designed to give 20,000-pound thrust at a chamber pressure of 300 lb/sq in. abs and sea-level exhaust. Showerhead type injectors were used. Data were obtained at chamber pressures of 300, 150, 125, and 100 lb/sq in. abs over a mixture range from 10 to 23 percent fuel. Specific impulse for all pressures ranged from 93 to 98 percent of the theoretical for equilibrium expansion. The highest value obtained was 335 pound-seconds per pound at 300 lb/sq in. abs and 22 percent fuel. Average overall heat-transfer rates varied from 2.0 to 6.3 Btu/(sq in.)(sec) and closely matched calculated values. The experiments totaled 13 minutes of operation with chambers constructed of stamped channels which were brazed and wrapped with wire. Damage to the inner walls was experienced only during runs at 300 lb/sq in. abs.

Low-frequency oscillations (approx. 100 cps) were obtained during operation at 100 to 150 lb/sq in. abs. These oscillations did not cause chamber damage. Sound recordings indicated the possibility of high-frequency oscillations at a chamber pressure of 300 lb/sq in. abs.

INTRODUCTION

The very high specific impulse of the hydrogen-oxygen combination makes it of great interest for space vehicles. Theory indicates it to be only about 4 percent below hydrogen with fluorine, the highest among stable chemical combinations. However, with oxygen, the handling problems implicit in the extreme reactivity and toxicity of fluorine are avoided. The unique physical properties of hydrogen make it an excellent coolant and fuel. These factors make the development of lightweight regeneratively cooled hydrogen-oxygen thrust chambers very desirable.

*Title, Unclassified.

This investigation was conducted primarily to determine problems involved in a lightweight regenerative thrust chamber of practical size and configuration using hydrogen and oxygen. The principal factors of interest were:

(1) Demonstration of high combustion efficiency in a regenerative engine with liquid hydrogen and oxygen. An investigation preliminary to this one (ref. 1) showed high efficiency with gaseous hydrogen and liquid oxygen in uncooled chambers with similar injectors.

(2) The comparison of measured overall heat-rejection rates with those calculated by pipe-flow formulas and variations of heat rejection circumferentially in the chamber

(3) Stability of operation over a wide range of conditions

(4) The effect on performance, stability, and heat flux of reduced chamber pressure and injector pressure drops

(5) Problems encountered with lightweight hardware under stress at high heat fluxes, steep temperature gradients, and repeated wide-range temperature cycling

The regeneratively cooled chambers used were designed to give 20,000 pounds thrust at 300 lb/sq in. abs chamber pressure. Showerhead injectors were used. Runs were made at chamber pressures of 300, 150, 125, and 100 lb/sq in. abs. The hydrogen in the propellant was varied from 10 to 23 percent. Experimental specific impulse, characteristic velocity, thrust coefficient, and overall heat-rejection rate are shown as functions of percent fuel for each chamber pressure and compared with the theoretical values. Data obtained on other thrust-chamber problems are presented and discussed. Among these are combustion pressure oscillations, circumferential heat-transfer variations, and structure design and material problems.

EQUIPMENT AND PROCEDURE

Facility

This investigation was conducted at the rocket engine research facility of the Lewis Research Center. A general description of the facility is given in reference 1.

The liquid-oxygen and liquid-hydrogen systems were essentially conventional pressurized systems. A high-pressure gaseous-fluorine system

was used for engine ignition. The arrangement of the propellant systems and test stand is shown in figure 1. Figure 2 is a schematic drawing to scale of the thrust chamber assembled on the test stand with its associated plumbing. The stand is essentially that used in reference 1 with the appropriate plumbing changes necessary to accommodate a regenerative chamber.

Propellants

Liquid hydrogen, gaseous hydrogen, liquid oxygen, and liquid fluorine were obtained from commercial suppliers. The hydrogen and oxygen were at least 99.5 percent pure. Fluorine purity was 99 percent.

Test Procedure

Engine operational functions were controlled by means of an electrical sequence timer. A 3- to 4-second hydrogen lead was used to assure a steady temperature of about 45° R at the inlet to the coolant manifold. Fluorine gas was then introduced into the chamber through the oxygen injector dome and tubes and it ignited the hydrogen. The oxygen valve was then opened. Chamber pressure buildup was coincident with oxygen flow buildup and took about 3/4 second. Ignition with this system was smooth and reliable, as reported in reference 2. After full thrust was achieved, an automatic controller was programmed in to control fuel and oxidant flow. The controller responded to feedback from the propellant flows and chamber pressure and acted to maintain constant fuel concentration and chamber pressure; during some runs, step changes in fuel percent were made at constant chamber pressure. Shutdown was accomplished with a short hydrogen override to prevent chamber overheating.

Engines

Thrust chambers. - The chambers used in this investigation are illustrated in figure 3. The chambers were designed to deliver 20,000 pounds thrust at 300 lb/sq in. abs chamber pressure. The contraction area ratio was 1.90, and the expansion area ratio was 3.68. The chambers consisted essentially of 120 stamped nickel or stainless steel channels assembled on a mandrel and brazed together to form the engine inner contour and coolant passages.

The channels were precision ground to give a predetermined variation of coolant passage height along the engine. Channel heights were designed such that calculated wall temperatures never exceeded 1000° F at any operating condition. Fully developed turbulent pipe flow formulas were used as outlined in reference 3.

The outside wall of the chamber was formed of high-strength stainless steel wire spiral wound over the channels and brazed to the channels and itself. Appropriate manifolds and flanges completed the engine.

Injectors. - The injectors used in this investigation were converging showerheads. Both the fuel and oxidant jets were drilled so as to allow the propellant streams to meet at a common point 20 to 23 inches from the injector face. Each injector consisted of a face plate containing the injection holes, a fuel distribution plate which apportioned the fuel across the back of the face plate to provide uniform cooling, and oxidant tubes and a back plate to distribute and inject oxidant. Two types of injectors were used. They differed only in number and size of jet holes, shape of face plate, and method of construction.

Figure 4 shows the face plate of a lightweight injector built of nickel stampings and thin-wall nickel tubes. The plates were concave, and all the jet holes were drilled normal to them so as to impinge 20 inches from the face. There were 1353 oxidant tubes evenly distributed over the face, each terminating in a 0.031-inch jet hole. The 2628 0.052-inch hydrogen holes were arranged so as to surround the oxidant holes uniformly. In addition, 180 0.031-inch hydrogen holes were uniformly spaced around the outer edge for injector rim cooling. This type of injector is designated injector A. An injector used for one series of tests at 150 lb/sq in. abs had two such rows of 180 holes. This injector was designated A modified. The upstream side of the face plate was chemically milled to provide hydrogen cooling passages. The entire assembly was furnace brazed together.

Figure 5 shows a face view of injector B. This injector had a flat face and was identical to that used in reference 1 except that the jet holes converge to a point 23 inches from the face. The face plate, fuel distribution plate, and oxidant tubes were machined from copper. There were 553 0.043-inch oxidant injection holes and 1160 0.067-inch fuel injection holes.

Figure 6(a) shows the flow paths for hydrogen, oxygen, and the gaseous-fluorine ignitor. Injector A is shown, but the paths also apply to injector B. Oxygen and fluorine entered the injector directly from their supply lines, while hydrogen first passed through the coolant jacket. Figure 6(b) shows the paths for hydrogen cooling the injector face.

Instrumentation

Thrust. - Thrust was measured with strain-gage load cells. One cell was located under each of the three thrust-stand legs (fig. 2), and

the electrical outputs were summed and recorded on a self-balancing potentiometer. Calibrations indicated a probable error of 0.6 percent.

Pressures. - Chamber pressure, propellant injector pressures, flowmeter pressure drops, and engine coolant jacket pressure drop were all measured with temperature-compensated strain-gage pressure transducers. The output of each was recorded on either a self-balancing potentiometer or a direct-reading oscillograph. At steady-state conditions the probable error in the pressure measurements was about 3/4 percent. Dynamic response of the chamber pressure measuring system was adequate to follow low-frequency oscillations up to about 200 cycles per second.

Flow rates. - Oxidant flow was measured with a Venturi flowmeter, calibrated in the system with liquid oxygen as in reference 1. The flowmeter, the tank, and most of the line were immersed in liquid nitrogen to maintain uniform temperature. The probable error in flow measurements, including density determinations, was less than 1.25 percent.

Hydrogen flow was measured with a Venturi flowmeter mounted in the dip tube of the supply tank to minimize hydrogen property variation. The probable error in hydrogen flow measurement was approximately 2 percent, including density determination.

Temperatures. - Oxidant temperatures at the flowmeter and the injector were measured with copper-constantan thermocouples that recorded on self-balancing potentiometers. The probable error was approximately 2° F.

The hydrogen temperatures in the propellant tank and flow line were measured using carbon resistors and self-balancing potentiometers to a precision of about 1° F. Hydrogen temperatures at the coolant jacket outlet were measured with 16 copper-constantan thermocouples uniformly spaced circumferentially and were recorded on a recording oscillograph. The probable error of determination was approximately 5° F.

Sound recording. - Sound recordings were taken in the test cell about 10 feet from the engine, which was sealed into an exhaust duct. The microphone and tape recorder combination used gave a response of ± 3 decibels from 200 to 8000 cycles per second.

RESULTS AND DISCUSSION

Performance

The performance data are presented in table I and figure 7. The theoretical performance values for all chamber pressures were calculated for constant area ratio and ambient pressure and include the effects of

overexpansion, underexpansion, and exhaust separation where applicable. No corrections were made for either exhaust-nozzle divergence or thermodynamic unavailability due to the low contraction ratio.

Figure 7(a) shows specific impulse (I_s), characteristic velocity (C^*), and thrust coefficient (C_F) for injectors A and B at a chamber pressure of 300 lb/sq in. abs. High performance is indicated for injector B (94.4 percent of theoretical equilibrium specific impulse at around 12 to 14 percent fuel, rising to 96 percent at 18 to 22 percent fuel). At 15 percent fuel, specific impulse was 321 pound-seconds per pound or 95 percent of the equilibrium theoretical. These data indicate specific-impulse efficiency within 1 percent of that obtained previously using a similar injector with gaseous hydrogen and liquid oxygen in an uncooled engine (ref. 1). Somewhat lower performance was obtained with injector A, approximately 93 percent of theoretical from 12 to 16 percent fuel. Specific impulse was 314 pound-seconds per pound at 15 percent fuel.

The difference in performance between injectors A and B is apparently due to differences in fuel distribution. Injector A had about 2 percent of the hydrogen flow in a ring of axial holes about 3/4 inch from the main pattern. Since this hydrogen was not uniformly mixed into the main stream in the chamber, the probability of the oxygen's completely reacting would be lowered. Without this cooling ring, injector A would be expected to give slightly higher performance than B because of smaller holes and finer distribution. However, in a chamber of this length, differences due to propellant atomization are minimized.

The C^* and I_s data show the same trend. The C_F curve is essentially flat. However, the positions of the two curves relative to their respective theoreticals (C^* is low; C_F is high) indicate a systematic discrepancy in determining the true chamber pressure, that is, the total pressure in the nozzle.

The chamber pressure was calculated from the pressure measured in the chamber at the injector and took into account the nonisentropic acceleration of the gases through the chamber and the high injection momentum. Uncertainties in these calculations may have accounted for the lower than anticipated chamber pressure. On the other hand, injector end pressure measurement may have been influenced by some unknown factor such as aspiration around the pressure tap due to high-velocity hydrogen jets. Data for C^* and C_F for four of the injector A runs are not shown because of a suspected error in injector end pressure measurement. (These data are tabulated but not plotted.)

Figure 7(b) shows I_s, C^*, and C_F for injector A at 150 lb/sq in. abs chamber pressure. Specific impulse is consistently high (96 percent of equivalent theoretical) for 10.4 to 15 percent fuel. The

specific impulse at 15 percent fuel was 284 pound-seconds per pound. However, above 15 percent, the efficiency drops uniformly to 93.5 percent of equilibrium and stays at this value to 23 percent fuel. This is in contrast to data obtained at 300 lb/sq in. abs using injectors of type B, both in regenerative chambers with liquid hydrogen and in uncooled chambers with gaseous hydrogen. These data indicated highest efficiency in the fuel-rich region. The C^* data show the same trend as I_s. The C_F curve is similar in shape to the equilibrium theoretical. Again, as at 300 lb/sq in. abs, a systematic discrepancy in chamber pressure determination is implicit from the positions of the C^* and C_F curves.

Data for tests in which considerable hydrogen leaked past the chamber-injector seal into the chamber are also shown. A considerable drop in performance is indicated. Data for C^* show a drop in combustion efficiency, apparently due to very poor propellant distribution; C_F also dropped, probably because of severely striated flow. Both of these effects were most evident at low fuel percents, where the probability of all the oxygen reacting with the poorly distributed hydrogen is lowest.

Figure 7(c) shows I_s, C^*, and C_F for injector A at a chamber pressure of 125 lb/sq in. abs. Specific impulse varies from 99 percent of theoretical at 14 percent fuel to 96 percent at 19 percent fuel. Specific impulse was 274 pound-seconds per pound at 15 percent fuel, which is 98 percent of the theoretical for equilibrium expansion. The trend is similar to that at 150 lb/sq in. abs, but the level is slightly different. However, at this pressure level with incipient exhaust-nozzle flow separation indicated, accurate calculation of theoretical thrust is difficult. The C^* data show the same trend as I_s, and C_F parallels the theoretical curve for separated flow based on equilibrium conditions. As at 150 lb/sq in. abs (but to a lesser extent), the general level of chamber pressure seems low.

Figure 7(d) shows I_s, C^*, and C_F for injector A at 100 lb/sq in. abs. The performance trends are similar to those at 150 and 125 lb/sq in. abs, falling efficiency at higher fuel percents. However, the combustion efficiency remains high even though the injector pressure drops are only 15 lb/sq in. for oxygen and 30 lb/sq in. for hydrogen. At this pressure, separation is fully developed over the whole mixture range and the theoretical thrust can be more accurately determined. The specific-impulse efficiency compares closely with that obtained at 150 lb/sq in. abs chamber pressure. At 15 percent fuel, efficiency was 96 percent and specific impulse 256 pound-seconds per pound.

Cooling

Average heat flux. - Variations of overall heat fluxes with mixture ratio are shown for chamber pressures of 300, 150, 125, and 100 lb/sq in. abs in figure 8. The experimental values in these plots were computed from measured hydrogen weight flows and temperature rises. At 15 percent fuel, the average heat flux was 6.1 Btu/(sq in.)(sec) at 300 lb/sq in., 3.0 at 150, 2.8 at 125, and 2.3 at 100. The calculated values shown in the figures were from fully developed turbulent flow equations for tubes and were based on measured propellant flow rates, coolant inlet pressures, and coolant inlet temperatures; gas temperatures were calculated from the theoretical temperatures using experimental C^* efficiencies. A high-speed computer program similar to that of reference 3 was used.

Agreement between experimental and calculated data is generally within 15 percent, except near stoichiometric for 150 lb/sq in. abs. In this region calculated values show considerable increase with decreasing percent fuel, but experimental values do not follow the trend. The 4 percent hydrogen used for rim cooling with injector A modified at 150 lb/sq in. abs resulted in lower heat fluxes than were obtained in injector A with 2 percent hydrogen (fig. 8(b)).

These data show that pipe-flow formulas can be used to obtain good approximations of the overall heat rejection to the thrust chambers. How well those formulas approximated the heat rejection at different locations along the length of the chambers could not be determined from these experiments. It is well known that propellant injection can have significant effects on local heat rejection, particularly in the combustion chamber, which would not be predicted by pipe-flow formulas. Some effects of this nature occurred in these experiments and are discussed in the following section.

Temperature distribution at cooling-jacket outlet. - Coolant temperatures measured at 16 locations in the jacket outlet showed wide peripheral variations. Figure 9 shows two typical sets of such data taken at 150 lb/sq in. abs with 11.3 (nearly stoichiometric) and 15.2 percent fuel. The temperature distribution plots have been superimposed on a photograph of injector A in the proper relative position. Three factors can be seen in figure 9, namely, the symmetry of the temperature patterns, the apparent relation between these patterns and that formed by the fuel and oxidant holes in the injector face plate, and the magnitude of peripheral temperature differences. Circumferential variations in propellant injection apparently produced corresponding variations in heat transfer due to changes in the boundary layer.

The symmetry of the coolant temperature patterns is typical of data obtained at all chamber pressures and mixture ratios investigated. Four

peaks of about the same magnitude roughly 90° apart were observed at each condition. The type of injection pattern used resulted in lack of symmetry at the outer edge. Blending of the square type pattern into the round edge resulted in a series of flat and stepped regions, as can be seen in figure 9. In general, the lowest coolant discharge temperatures were opposite the four wider flat spots on the rim, and the hottest temperatures were in between those areas and in the stepped regions. Injector B differed from A (fig. 9) only in that it had a coarser pattern. The same general relation between coolant temperature and rim pattern was observed with each. Peripheral differences in coolant discharge temperatures were greater at the stoichiometric condition (11.3 percent fuel) than with 15.2 percent fuel, since a smaller quantity of coolant had to remove a greater amount of heat and differences were correspondingly magnified. At the 11.3-percent-fuel condition the coolant temperature rises vary from roughly 100° to 250° F. The 250° F maximum exceeds the average over the entire periphery by about 30 percent.

E-625

The implications of peripheral variations in coolant temperature rises are significant. Consider the case at 11.3 percent fuel and 150 lb/sq in. abs chamber pressure. If temperature rises from point to point along the entire length of the channel were increased by 30 percent, the average increase in heat flux along that length within the combustion chamber would amount to 25 percent. However, if the 30-percent above-average temperature rise were assumed to be due to an effect which was limited to the combustion chamber, the corresponding average increase in heat flux would be 63 percent. This was calculated to result in a rise in gas-side wall temperature from 740° to 1210° F at a point 2 inches from the injector.

CI-2

At higher chamber pressures higher heat fluxes are encountered. However, because of the increased hydrogen flow rates in the fixed cooling passages, the chamber walls should be cooled to a greater degree at any given mixture ratio. The observed coolant temperature-rise distributions at 300 lb/sq in. abs were comparable with those obtained at 150 lb/sq in. abs at the same mixture ratios. Percentagewise, the peak-to-average coolant temperature rise was much the same. Calculations were made at 12.3 percent fuel (close to the leanest operating conditions at 300 lb/sq in. abs) to determine the effect of a 63-percent increase in combustion-chamber heat flux. The increase in heat flux and heat-transfer coefficient necessary to force the gas-side wall temperature to the melting point of nickel was also calculated. At a point 2 inches from the injector, it was found that a 63-percent increase in heat flux gave a 77-percent increase in the gas-side heat-transfer coefficient and increased the gas-side wall temperature from 355° to 720° F. In order to attain a gas-side wall temperature of 2620° F (melting point of nickel), an increase of roughly 400 percent in heat flux and of 900 percent in gas-side heat-transfer coefficient would be required.

[redacted]

Sufficient care was taken in designing the inlet to the cooling jacket to rule out that area as a source of any noticeable maldistribution of fuel (fig. 3). Any maldistribution arising from this source might be expected to be twin-lobed and symmetrical about the two inlets to the fuel manifold feeding the coolant channels. Instead, the pattern shown in figure 15 was observed and the symmetry was with respect to the injectors.

Condition of chambers. - Operation of two chambers, one nickel (233 sec) and one stainless steel (376 sec), for a total of 609 seconds at chamber pressures from 100 to 150 lb/sq in. abs was accomplished with only minor pin-hole leaks occurring in the coolant channels. Such leaks caused no difficulty during operation and were easily repaired. During experiments at 300 lb/sq in. abs, however, extensive damage occurred in four different chambers, three nickel and one stainless steel. Running time totaled 165 seconds with the longest run being 49 seconds. In general, there were local failures in the inner wall showing overstress and elevated temperatures. The channels of the nickel chambers were bulged into the combustion chamber; some showed cracks through the wall at the center of the span, while others had burst into the chamber for a short distance along their length (fig. 10). The wall failures occurred in areas having the same circumferential position as the measured peaks in hydrogen outlet temperature (fig. 9). No surface melting was observed. After three very short runs (2 to 4 sec) one of the nickel chambers not only had many burst channels but showed melting of the walls and the injector face. Much of the damage undoubtedly resulted from reduced local coolant flow following the initial failure. The chamber made with stainless steel, however, had much less damage than the nickel chambers despite much longer operation. Damage was limited to minor cracking without bulging or bursting. Although stainless steel has lower thermal conductivity and hence reaches higher temperatures, its greater strength would explain its greater resistance to damage. In no engine did the damage extend beyond the inner wall.

Detailed knowledge of conditions at which failures occurred is lacking for four reasons: (1) Actual wall temperatures reached during the experiments are unknown, although calculated wall temperatures (as discussed in the preceding section) are well below 1000° F for all cases at 300 lb/sq in. abs. (2) The physical properties of the nickel after fabrication are not well known because of such variables as the effect of repeated brazing cycles and possible grain boundary impurities and because properties are affected by high rates of heating such as encountered in the operation of the chambers. (3) Prediction of the

stresses in the walls from the combined effects of pressure differences and large thermal gradients is difficult in the structure formed by the channels and wire wrapping. (4) Sound recordings suggested the presence of high-frequency oscillations which may have produced locally damaging effects.

Bench tests were conducted with nickel channels to explore the problem of cracking. Attempts were made to approximate typical heating and loading conditions in the chambers. Channels in the as-formed condition prior to assembly and brazing were pressurized and subjected to rapid heating with an acetylene torch. Longitudinal cracking was observed when thermocouples indicated a wall temperature of 1800° F. The nickel in the engines was probably weaker because of repeated brazing cycles and may have failed at lower temperatures.

The following comparisons point to increased stress being associated with wall cracking rather than increased wall temperatures.

(1) The cracks described occurred only during operation at 300 lb/sq in. abs chamber pressure, for which pressure differences across the walls were several times those for operation at 100 to 150 lb/sq in. abs. Cooling calculations, however, predict lower wall temperatures for 300 lb/sq in. abs than for the lower chamber pressures.

(2) Cracks occurred in locations where channel span was greatest (combustion chamber and nozzle divergence), rather than where predicted wall temperatures were highest (throat and nozzle convergence).

(3) Smaller engines fabricated by the same method (5000-lb thrust at 300 lb/sq in., ref. 4) were operated at conditions resulting in predicted wall temperatures near melting. Melting occurred without indications of rupture due to overstress. Channel spans of the 20,000-pound-thrust chambers (which ruptured without reaching melting temperatures) were about 20 percent greater than for the smaller chambers and resulted in much higher stress.

It would appear from these observations that an increase in channel strength would be more significant in avoiding damage than a further increase in cooling, although elimination of hot streaks in the chamber is also desirable.

Deformation of injectors. - In figure 7(b), performance is presented for a condition in which there was considerable hydrogen leakage past the coolant-jacket - injector seal. This leakage resulted from injector shrinkage over a number of run cycles. A uniform shrinkage across the face of about 0.003 inch per inch per run cycle was observed with nickel type A injectors. Some warpage of the injector seal ring was also noted.

[redacted]

Both of these effects are believed to be due to yielding of the thin face and distribution plates under stresses resulting from unequal thermal expansions occurring in the injector because of large temperature gradients through the injector.

A simplified analysis of the injector stresses resulting from the engine operational cycle was made. This analysis indicated that deformation of the order encountered experimentally could be incurred as a result of the temperature cycling in the injector. The analysis also indicated that the deformation could continue indefinitely, as was the case experimentally.

Combustion Oscillations

Low-frequency oscillations. - Combustion pressure oscillations were encountered during operation at 100 to 150 lb/sq in. abs. They were generally intermittent, that is, rough periods alternated with smooth periods during a given run. The rough periods were characterized by pronounced oscillations in the oscillograph pressure traces, slightly increased coolant temperature rise, and a loud low-pitched sound. The combustion pressure frequencies were about 85 to 115 cycles per second. The amplitudes were about ±6 pounds per square inch absolute. The oscillations occurred during runs above 14 percent fuel. Operation at lower fuel percents was smooth. The oscillations did not cause any apparent damage to the thrust chambers used; however, a small drop in performance (less than 1 percent) was noted to accompany them. Overall heat-transfer increases of about 7 percent were noted during periods of rough running. Coolant pressure drops showed apparent increases of 10 to 20 percent during these periods.

Figure 11 is a portion of an oscillograph record showing pressure traces for a run in which intermittent low-frequency oscillations occurred. Operating conditions were: 150 lb/sq in. abs chamber pressure, 16 percent fuel, and 9000-pound thrust. A type A injector was used. The run duration was 102 seconds. A 100-cycle-per-second variation of ±6 lb/sq in. abs in chamber pressure was noted during some portions of this run. The cooling-jacket pressure drop and the fuel injection pressure also indicated oscillations occurring coincidently with the chamber pressure oscillations. The chamber pressure and fuel injection pressure measurements were calculated to be capable of dynamic response at the frequencies encountered; hence amplitudes recorded were felt to be meaningful. The oscillograph galvanometer recording cooling-jacket pressure drop, however, tended to resonance at these frequencies and had to be electrically damped.

The coincident oscillation of pickups in the hydrogen system with the chamber pressure suggests a link between hydrogen flow and chamber

pressure fluctuations. However, the data do not clearly indicate the nature of the oscillations. Several modes of oscillation are described in reference 5. The chamber itself may be inherently stable so that exterior perturbations will not excite nonsteady coordinating processes and result in organized oscillations. In general, a nondetrimental rough combustion will result. On the other hand, if a coordinating process is excited, organized oscillations of the rate-affecting factors or of injection rates can result. In this case, perturbations will be amplified and a detrimental oscillation will generally result.

The oscillations reported herein were of low amplitude. They may have been indicative of rough combustion driven by hydrogen flow fluctuations in the chamber cooling passages. Conversely, they may have been characteristic of combustion-chamber instability linked with hydrogen injection rate oscillations. Since the oscillations were apparently not damaging, nonlinear effects may have restricted amplitudes. Support for the latter hypothesis is derived from the observation that, while these oscillations were present at 100 to 150 lb/sq in. abs, they were not at 300 lb/sq in. abs. The runs at 300 lb/sq in. abs had a much greater ratio of injector pressure drop to chamber pressure and hence a lower sensitivity of flow rate to pressure fluctuations. In addition, combustion time delays estimated using the vaporization criteria of reference 6 were less for 300 lb/sq in. abs than for 100 to 150 lb/sq in. abs. Both of these effects tend to displace the 300 lb/sq in. abs data from the lower pressure data in the direction of stability. The increased stability at low fuel percents observed experimentally was not explained by the simplified analyses made.

High-frequency oscillations. - Sound recordings indicated increases of the order of 20 to 30 decibels in sound power levels for some runs, particularly at 300 lb/sq in. abs. These increases occurred over the whole mixture range tested with injector B and only above about 14 percent for injector A. Discrete peaks in sound amplitude were generally observed at frequencies between 3000 and 6500 cycles per second. This suggests the presence of high-frequency oscillations. Calculations show the first tangential mode of oscillation for this chamber to be approximately 3400 cycles per second at 15 percent fuel. The fundamental radial oscillation would be approximately 6900 cycles per second. The fundamental longitudinal frequency would be about 2400 cycles per second. However, the sound recordings alone do not permit verification of the existence of oscillations or identification of modes.

All the chamber wall failures occurred during runs in which the increased sound level was recorded. No distinct increases in overall heat rejection accompanied the increases in sound power level. However, oscillations may have produced locally damaging effects.

SUMMARY OF RESULTS

Experiments were conducted with hydrogen and oxygen in regenerative engines at chamber pressures of 300, 150, 125, and 100 lb/sq in. abs and at mixture ratios from 10 to 23 percent fuel. The thrust chambers were designed to give 20,000 pounds of thrust with expansion from 300 lb/sq in. abs to sea-level pressure. The injectors used were of the showerhead type. The results are as follows:

1. Specific impulse for all pressures ranged from 93 to 98 percent of the theoretical for equilibrium expansion. The highest value obtained was 335 pound-seconds per pound at 300 lb/sq in. abs and 22 percent fuel.

2. Durability of the thrust chamber over extended-duration testing was demonstrated at 150 lb/sq in. abs. Total running time for a single chamber was 380 seconds including a single run of 102 seconds with no engine damage. Run durations at 300 lb/sq in. abs were as long as 49 seconds; however, damage was encountered.

3. Evidences of low-frequency oscillations (approx. 100 cps) were noted during operation at 100 to 150 lb/sq in. abs. Although vibration amplitudes were low in all cases and no physical damage occurred, a small drop in performance was noted to coincide with the oscillations.

4. For some runs large increases in sound level were encountered, particularly at 300 lb/sq in. abs and at high fuel percents. Peak amplitudes were at frequencies from 3000 to 6500 cycles per second. No direct indentification of a particular instability mode was made.

Lewis Research Center
National Aeronautics and Space Administration
Cleveland, Ohio, January 11, 1960

REFERENCES

1. Rothenberg, Edward A., Kutina, Franklin J., Jr., and Kinney, George R.: Experimental Performance of Gaseous Hydrogen and Liquid Oxygen in Uncooled 20,000-Pound-Thrust Rocket Engines. NASA MEMO 4-8-59E, 1959.

2. Straight, David M., and Rothenberg, Edward A.: Ignition of Hydrogen-Oxygen Rocket Engines with Fluorine. NASA TM X-101, 1959.

3. Curren, Arthur N., Price, Harold G., Jr., and Douglass, Howard W.: Analysis of Effects of Rocket-Engine Design Parameters on Regenerative-Cooling Capabilities of Several Propellants. NASA TN D-66, 1959.

4. Douglass, H. W., Hennings, G., and Price, H. G., Jr.: Experimental Performance of Liquid Hydrogen and Liquid Fluorine in Regeneratively Cooled Rocket Engines. NASA TM X-87, 1959.

5. Crocco, Luigi, and Cheng, Sin-I: Theory of Combustion Instability in Liquid Propellant Rocket Motors. AGARDograph No. 8, Butterworths Sci. Pub. (London), 1956.

6. Priem, Richard J.: Propellant Vaporization as a Criterion for Rocket-Engine Design; Calculations of Chamber Length to Vaporize Various Propellants. NACA TN 3883, 1958.

TABLE I. - PERFORMANCE OF HYDROGEN AND OXYGEN

(a) Normal operation; chamber pressure, 300 lb/sq in. abs; injector A.

Fuel flow rate, lb/sec	Oxidant flow rate, lb/sec	Chamber pressure at injector, lb/sq in. gage	Thrust, lb	Percent fuel	Specific impulse, lb-sec/lb	Characteristic velocity, ft/sec	Thrust coefficient	Average engine cooling-jacket temperature change, °F	Overall heat transfer, Btu/(sq in.)(sec)	Pressure drop through cooling jacket, lb/sq in.	Fuel pressure drop through injector, lb/sq in.	Oxidant pressure drop through injector, lb/sq in.
8.33	61.0	294	20,700	12.0	299	6650	1.45	---	----	69	62	168
8.84	59.2	293	20,700	13.0	304	6770	1.45	---	----	---	---	165
9.18	61.1	290	21,300	13.1	304	6480	1.51	---	----	190	240	172
9.26	56.9	294	20,600	14.0	311	6970	1.44	---	----	92	67	140
9.28	56.0	278	20,200	14.2	309	6700	1.48	174	6.08	193	245	138
9.93	55.1	276	20,500	15.3	315	6700	1.51	167	6.32	203	247	145
10.49	54.0	277	20,500	16.3	317	6820	1.50	151	6.07	214	261	148

(b) Normal operation; chamber pressure, 300 lb/sq in. abs; injector B.

8.10	59.1	293	20,400	12.0	303	6900	1.41	180	4.99	---	---	---
8.63	57.9	291	20,700	13.0	311	6930	1.44	177	5.28	---	---	---
11.3	53.3	303	21,300	17.5	330	7400	1.44	155	6.14	193	---	242
12.6	51.0	302	21,400	19.9	336	7490	1.44	139	6.30	206	---	178
13.7	53.5	321	22,300	20.4	332	7540	1.42	129	6.29	217	166	221
14.2	49.9	304	21,500	22.2	335	7500	1.44	126	6.49	225	---	165

TABLE I. - Continued. PERFORMANCE OF HYDROGEN AND OXYGEN

(c) Normal operation; chamber pressure, 150 lb/sq in. abs; injector A.

Fuel flow rate, lb/sec	Oxidant flow rate, lb/sec	Chamber pressure at injector, lb/sq in. gage	Thrust, lb	Percent fuel	Specific impulse, lb-sec/lb	Characteristic velocity, ft/sec	Thrust coefficient	Average engine cooling-jacket temperature change, °F	Overall heat transfer, Btu/(sq in.)(sec)	Pressure drop through cooling jacket, lb/sq in.	Fuel pressure drop through injector, lb/sq in.	Oxidant pressure drop through injector, lb/sq in.
3.67	31.6	139	8950	10.4	254	6480	1.26	216	2.68	42	27	114
3.90	30.4	139	9030	11.4	263	6660	1.27	201	2.64	45	29	110
4.09	29.6	139	9110	12.1	270	6780	1.28	210	2.95	48	31	101
4.37	28.8	139	9150	13.2	276	6910	1.28	199	2.68	47	38	104
4.59	27.6	139	9070	14.2	281	7100	1.28	176	2.68	54	37	106
4.82	27.1	139	9070	15.1	284	7160	1.28	173	2.65	55	40	102
5.28	27.2	140	9130	16.3	282	7100	1.27	131	2.21	50	44	102
5.34	26.7	143	9060	16.7	283	7320	1.24	177	2.05	43	31	35
5.79	26.2	143	9080	18.1	284	7330	1.25	171	3.18	43	28	25
6.36	25.8	143	9080	19.8	283	7310	1.24	158	3.13	43	29	26
6.85	25.2	143	9080	21.4	284	7340	1.24	152	3.26	44	28	20
7.26	24.5	143	9060	22.9	285	7400	1.24	142	3.20	46	29	23

(d) Normal operation; chamber pressure, 150 lb/sq in. abs; injector A modified.

5.69	31.8	163	10,870	15.2	290	7060	1.32	199	3.50	47	61	40
5.19	28.2	157	9,690	15.5	290	7660	1.22	128	1.99	55	43	27
5.07	26.5	137	8,790	16.1	279	7170	1.25	128	2.16	49	64	39
5.38	27.8	155	9,390	16.2	283	7600	1.20	148	2.42	76	32	29

TABLE I. - Concluded. PERFORMANCE OF HYDROGEN AND OXYGEN

(e) Hydrogen leakage past cooling-jacket - injector seal into combustion chamber; chamber pressure, 150 lb/sq in. abs; injector A modified.

Fuel flow rate, lb/sec	Oxidant flow rate, lb/sec	Chamber pressure at injector, lb/sq in. gage	Thrust, lb	Percent fuel	Specific impulse, lb-sec/lb	Characteristic velocity, ft/sec	Thrust coefficient	Average engine cooling-jacket temperature change, °F	Overall heat transfer, Btu/(sq in.)(sec)	Pressure drop through cooling jacket, lb/sq in.	Fuel pressure drop through injector, lb/sq in.	Oxidant pressure drop through injector lb/sq in.
4.01	31.8	136	8310	11.2	232	6260	1.19	---	----	43	17	45
4.64	31.8	143	8790	12.7	241	6460	1.20	---	----	46	20	44
5.34	31.6	151	9300	14.5	252	6670	1.21	---	----	51	22	43
6.20	27.4	139	8920	18.4	265	6840	1.25	---	----	--	29	28
6.92	27.4	146	9320	20.2	272	6990	1.25	---	----	66	34	34
7.42	27.4	151	9640	21.3	277	7080	1.26	---	----	71	38	35

(f) Normal operation; chamber pressure, 125 lb/sq in. abs; injector A.

3.65	23.0	116	7240	13.7	272	7270	1.20	228	2.80	28	39	26
4.01	22.3	116	7220	15.3	275	7360	1.20	213	2.84	45	36	27
4.34	21.8	116	7200	16.6	275	7400	1.20	193	2.72	43	39	21
4.72	21.2	116	7240	18.2	279	7470	1.20	171	2.55	42	54	24
4.96	21.0	116	7240	19.1	278	7460	1.20	156	2.42	45	58	22

(g) Normal operation; chamber pressure, 100 lb/sq in. abs; injector A.

2.83	18.4	88	5280	13.3	248	7140	1.12	249	2.51	23	29	18
3.04	17.6	87	5300	14.7	256	7330	1.13	225	2.35	26	31	15
3.27	17.0	87	5240	16.1	258	7460	1.12	208	2.30	31	33	14
3.33	17.0	87	5240	16.4	257	7440	1.12	202	2.20	27	32	14
3.64	17.0	88	5220	17.7	253	7360	1.11	188	2.26	34	35	14
3.95	16.4	88	5300	19.4	260	7490	1.12	147	1.85	--	--	14

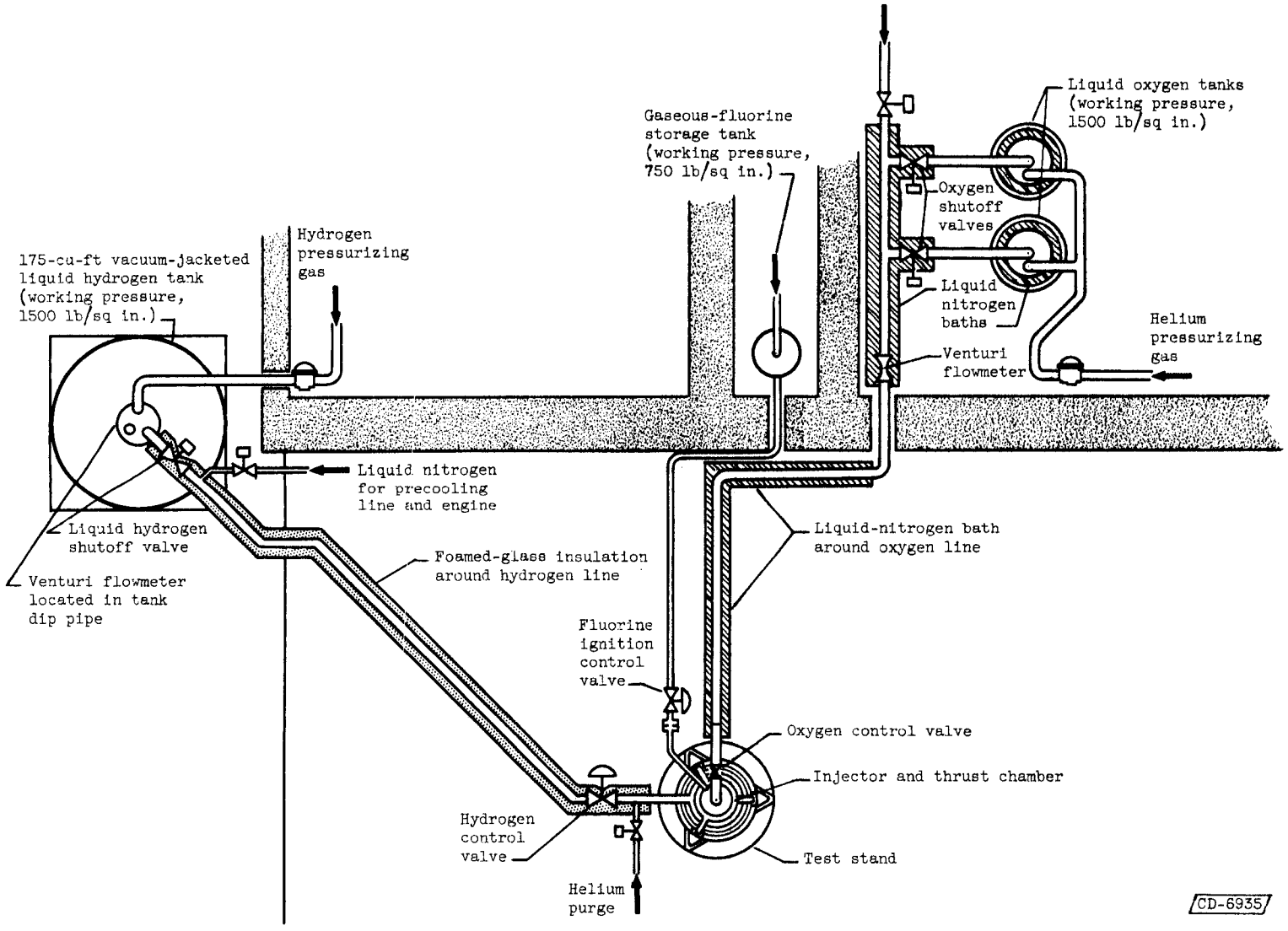

Figure 1. - Arrangement of hydrogen-oxygen propellant systems in test building.
Scale: 1 inch is approximately 13 feet.

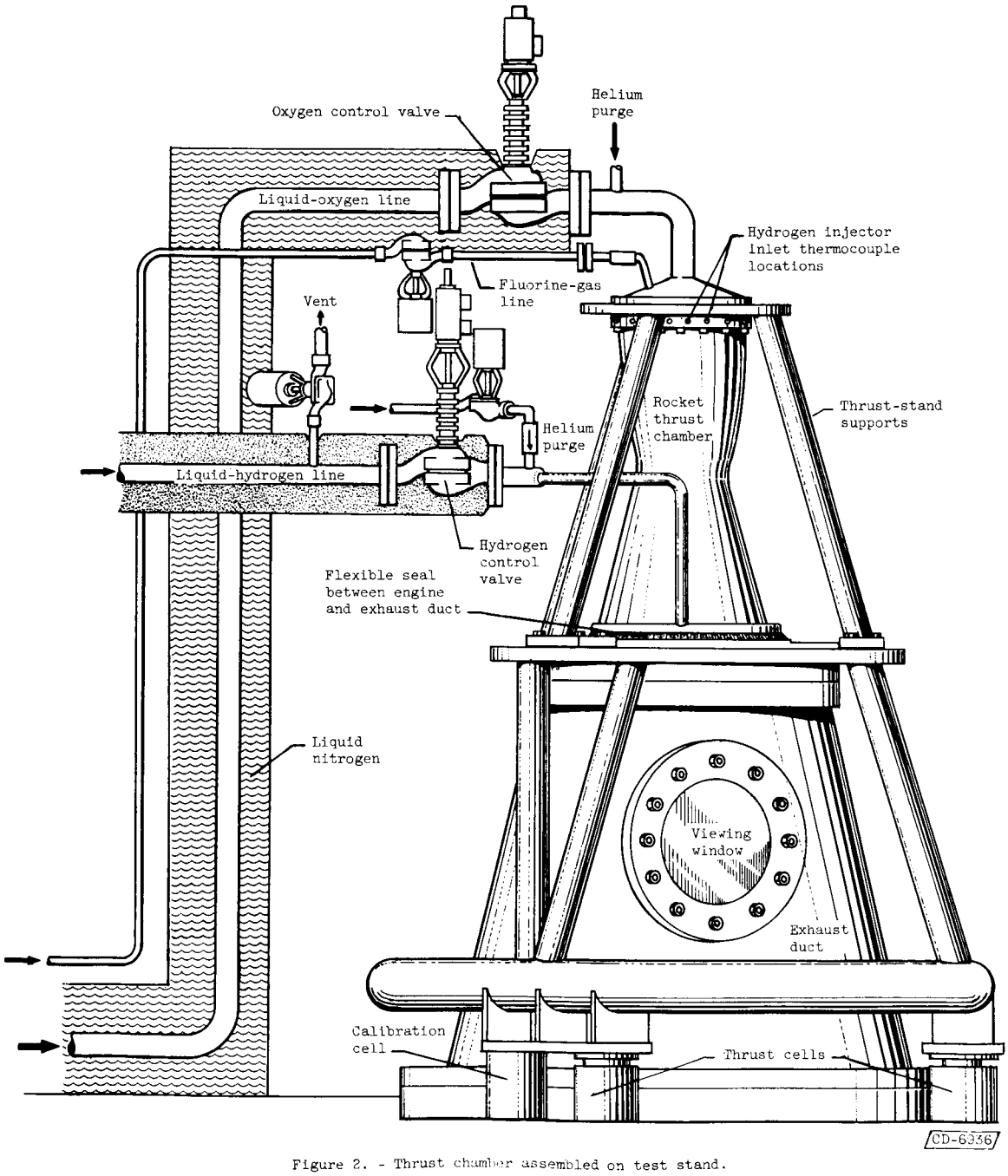

Figure 2. - Thrust chamber assembled on test stand.

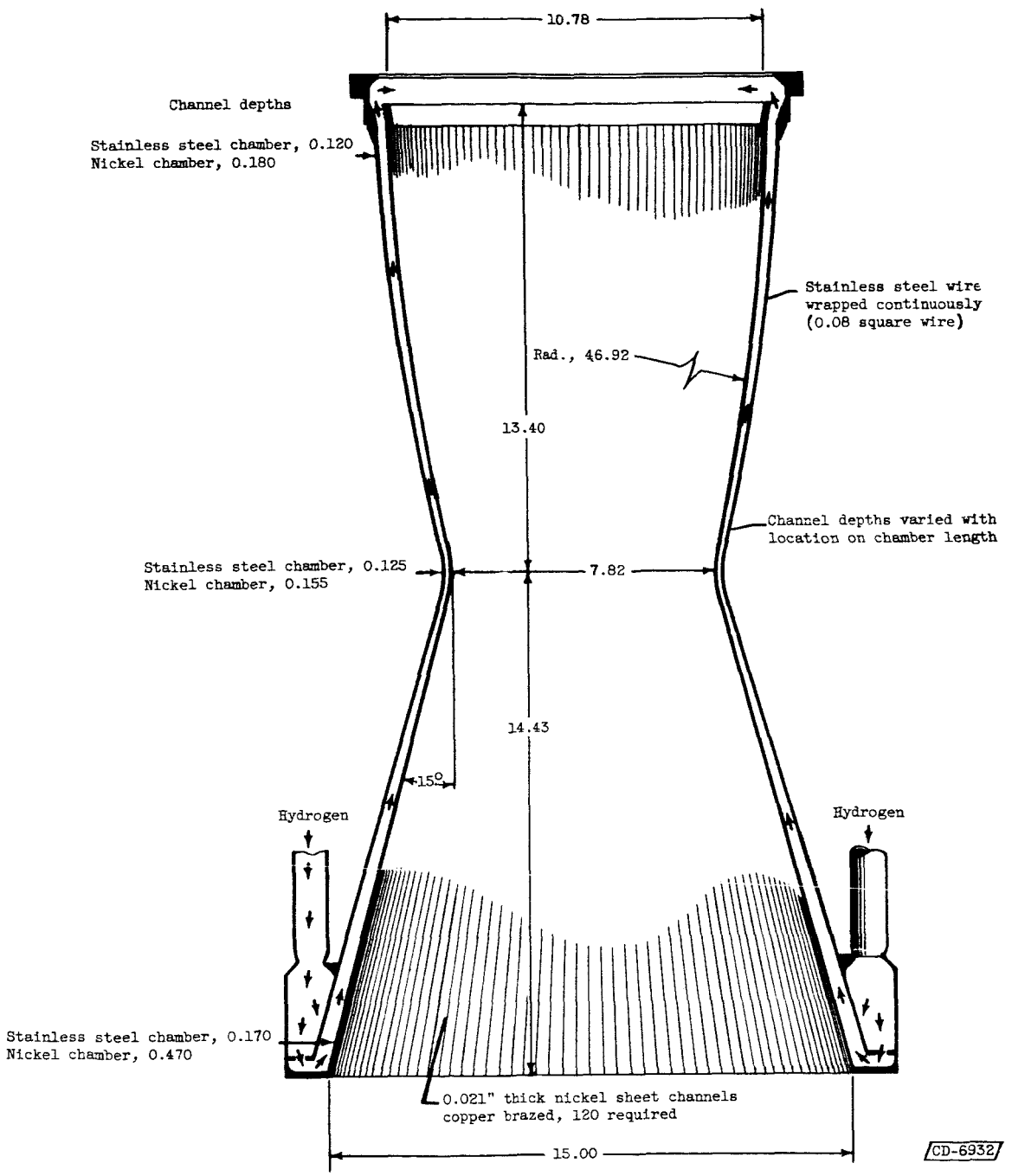

(a) Cross-sectional drawing. Scale, 1/4 inch equals 1 inch; all dimensions in inches.

Figure 3. - Regeneratively cooled 20,000-pound-thrust rocket chamber (chamber pressure, 300 lb/sq in. abs).

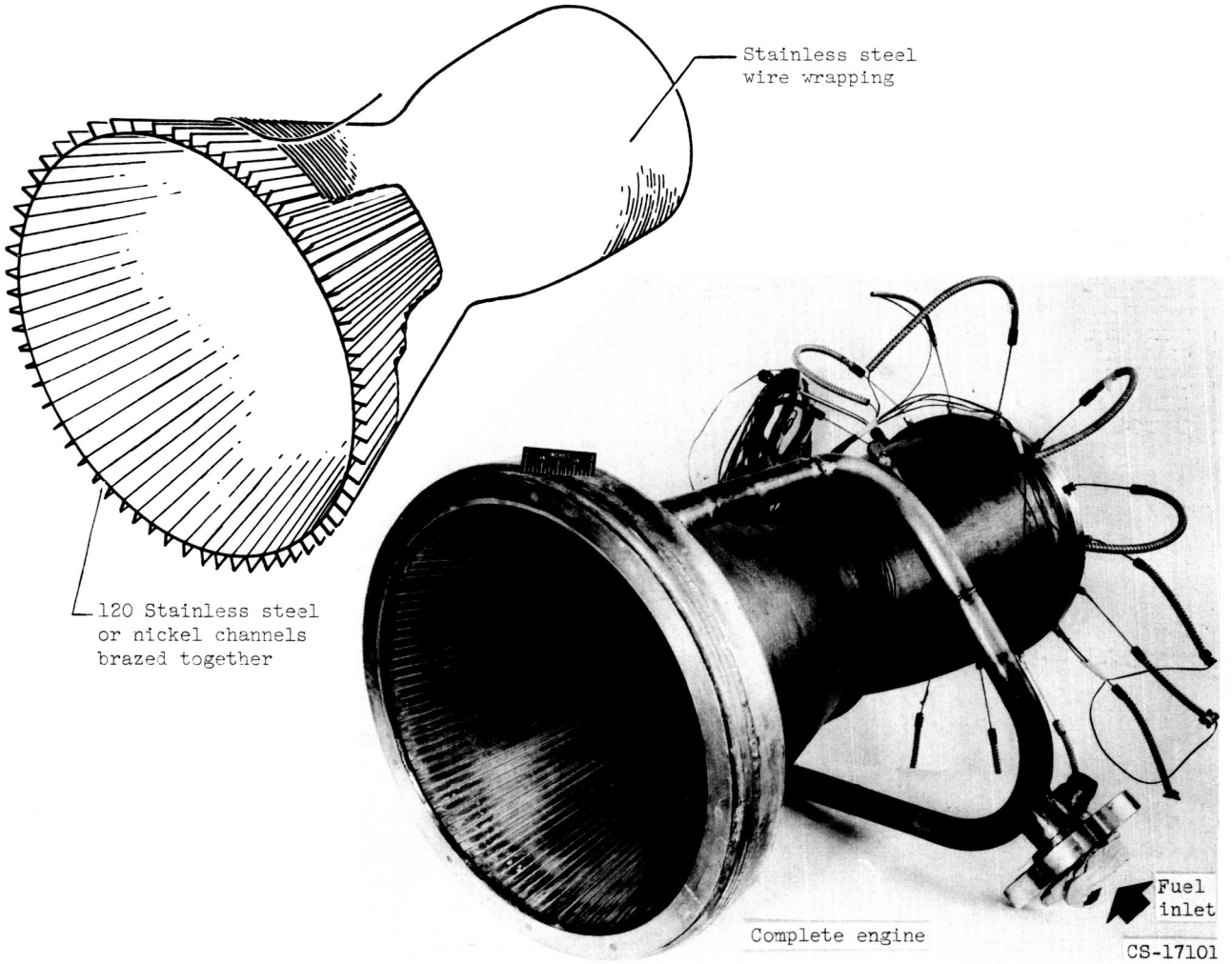

(b) Pictorial views.

Figure 3. - Concluded. Regeneratively cooled 20,000-pound-thrust rocket chamber (chamber pressure, 300 lb/sq in. abs).

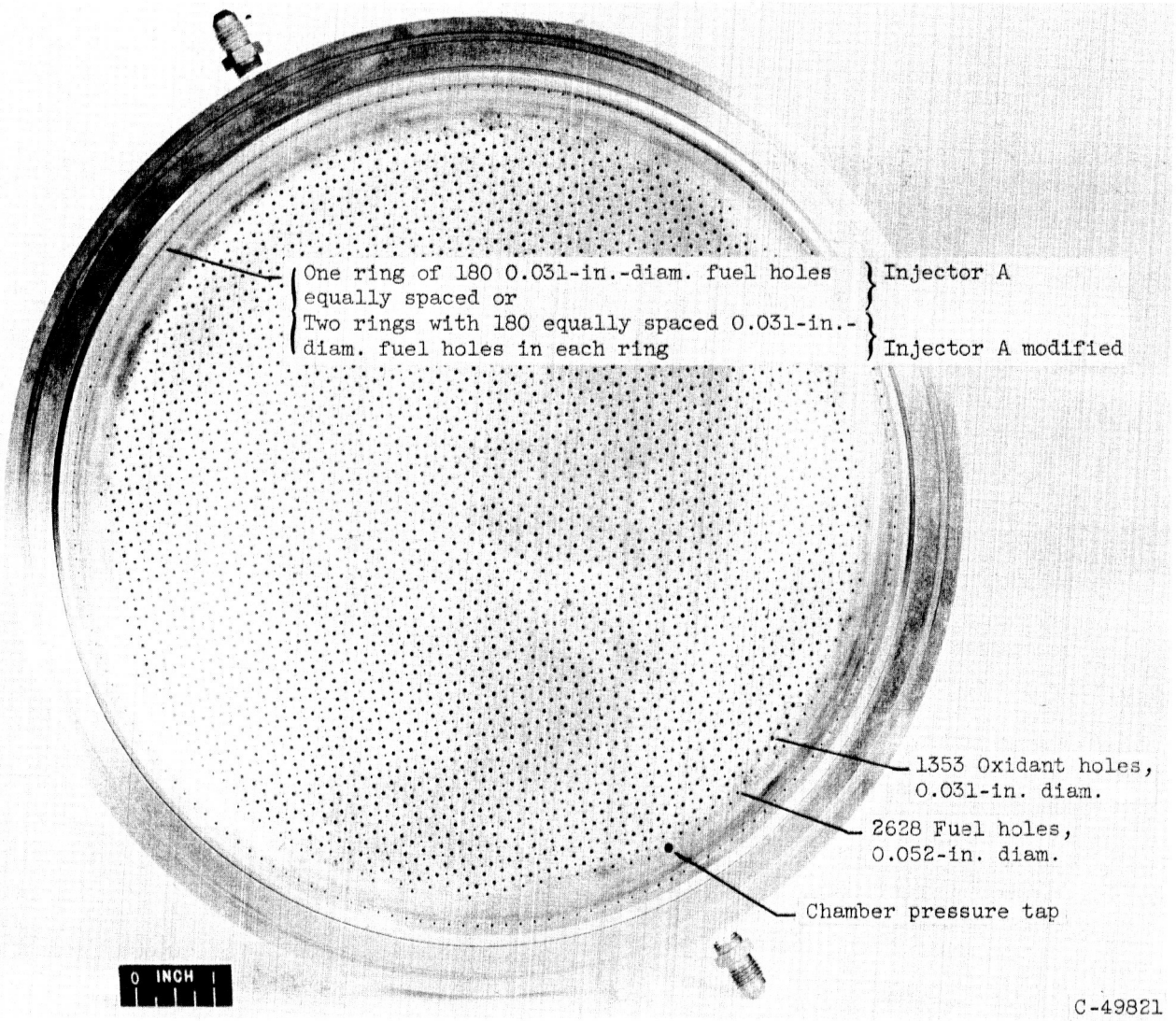

Figure 4. - Face view of lightweight nickel injector.

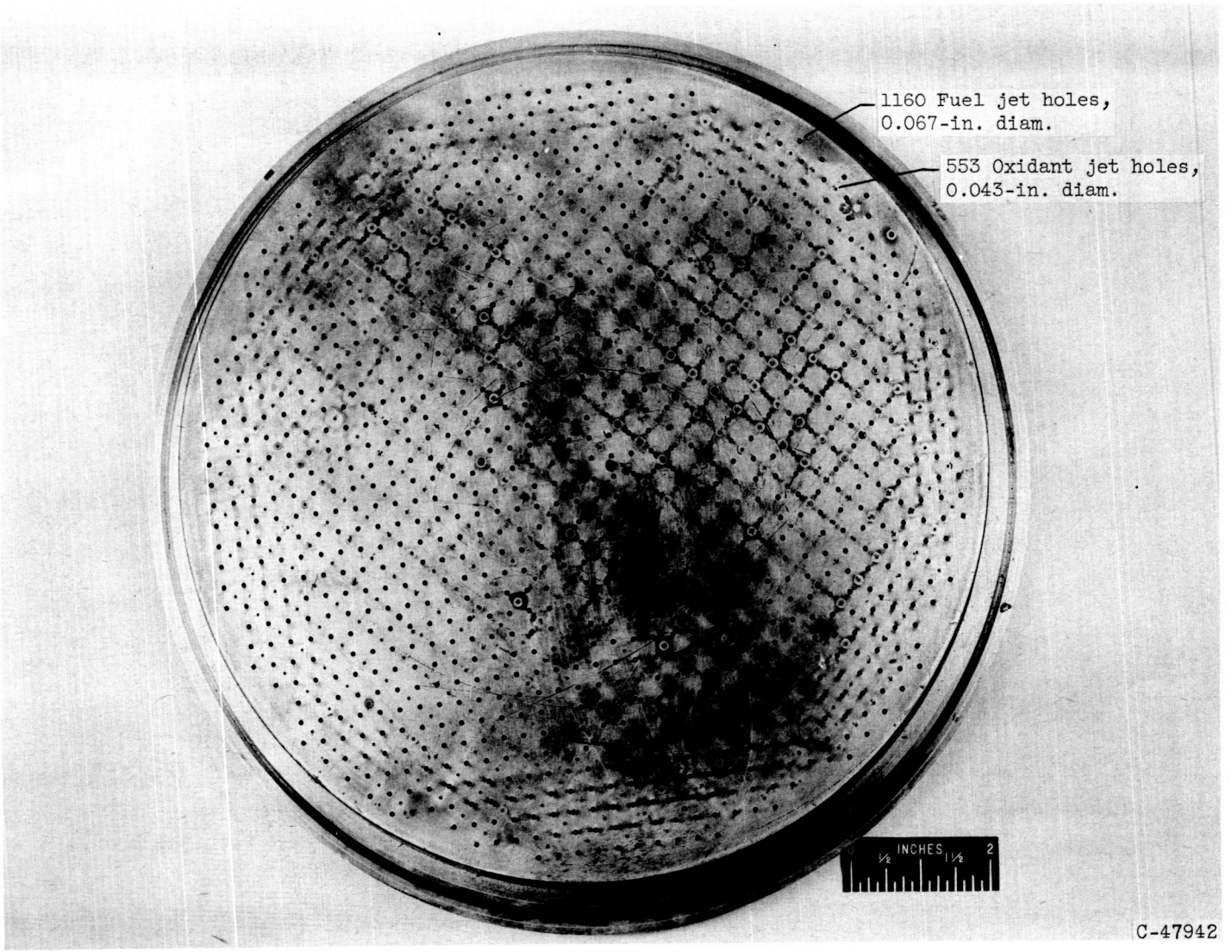

(Injector B).

Figure 5. - Face view of heavy-weight copper injector.

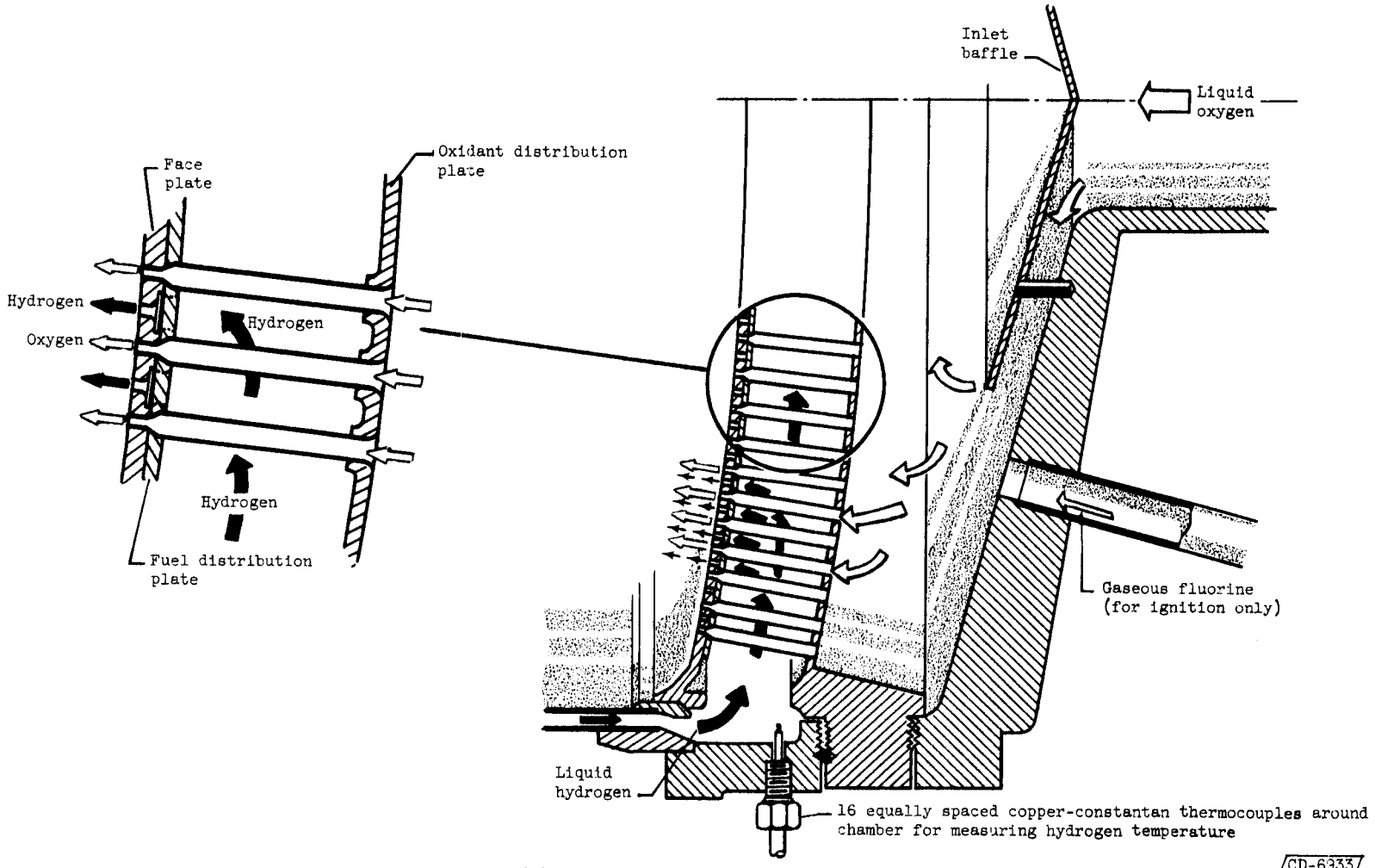

(a) Propellant flow paths.

Figure 6. - Cutaway views of injector.

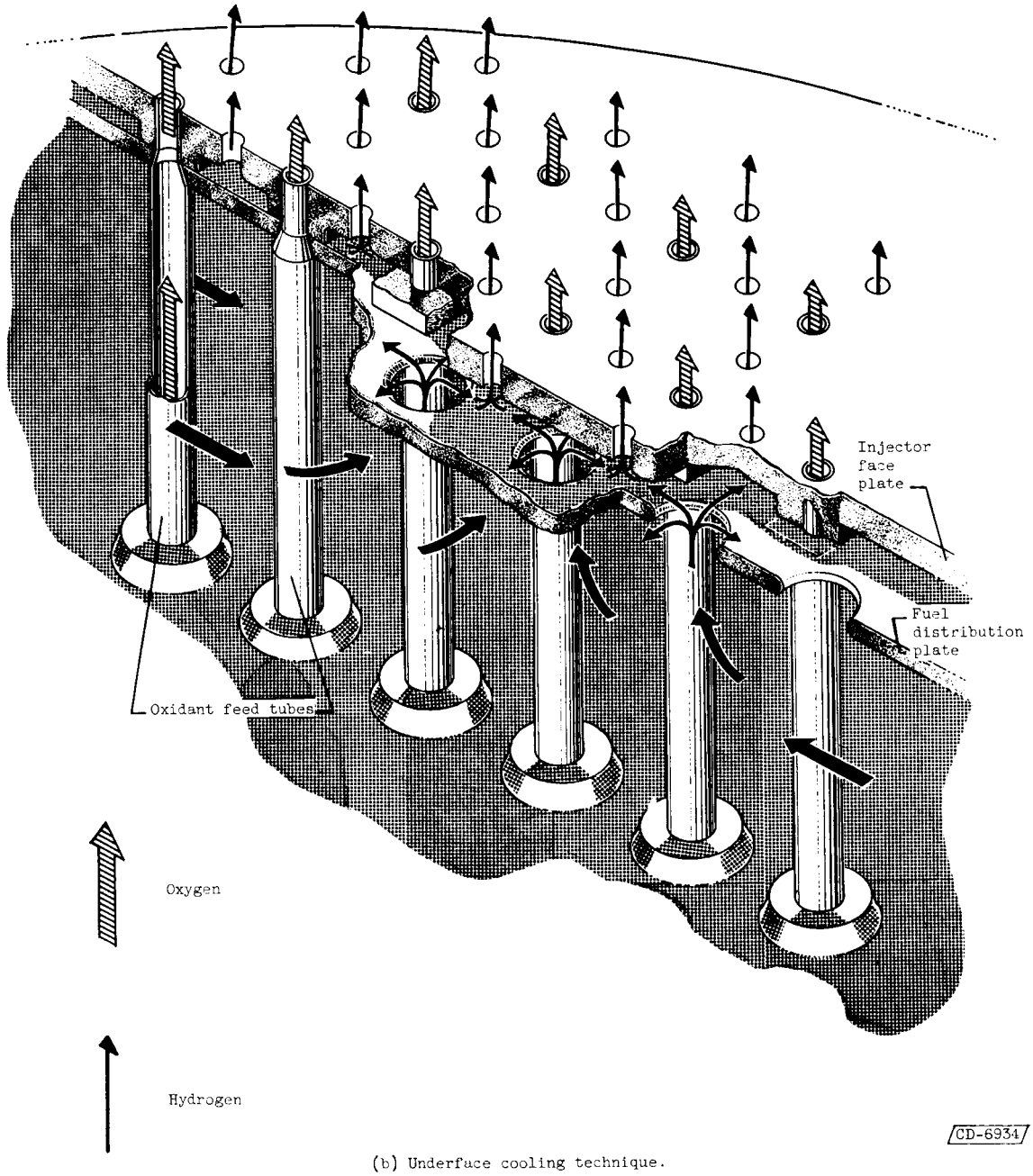

(b) Underface cooling technique.

Figure 6. - Concluded. Cutaway views of injector.

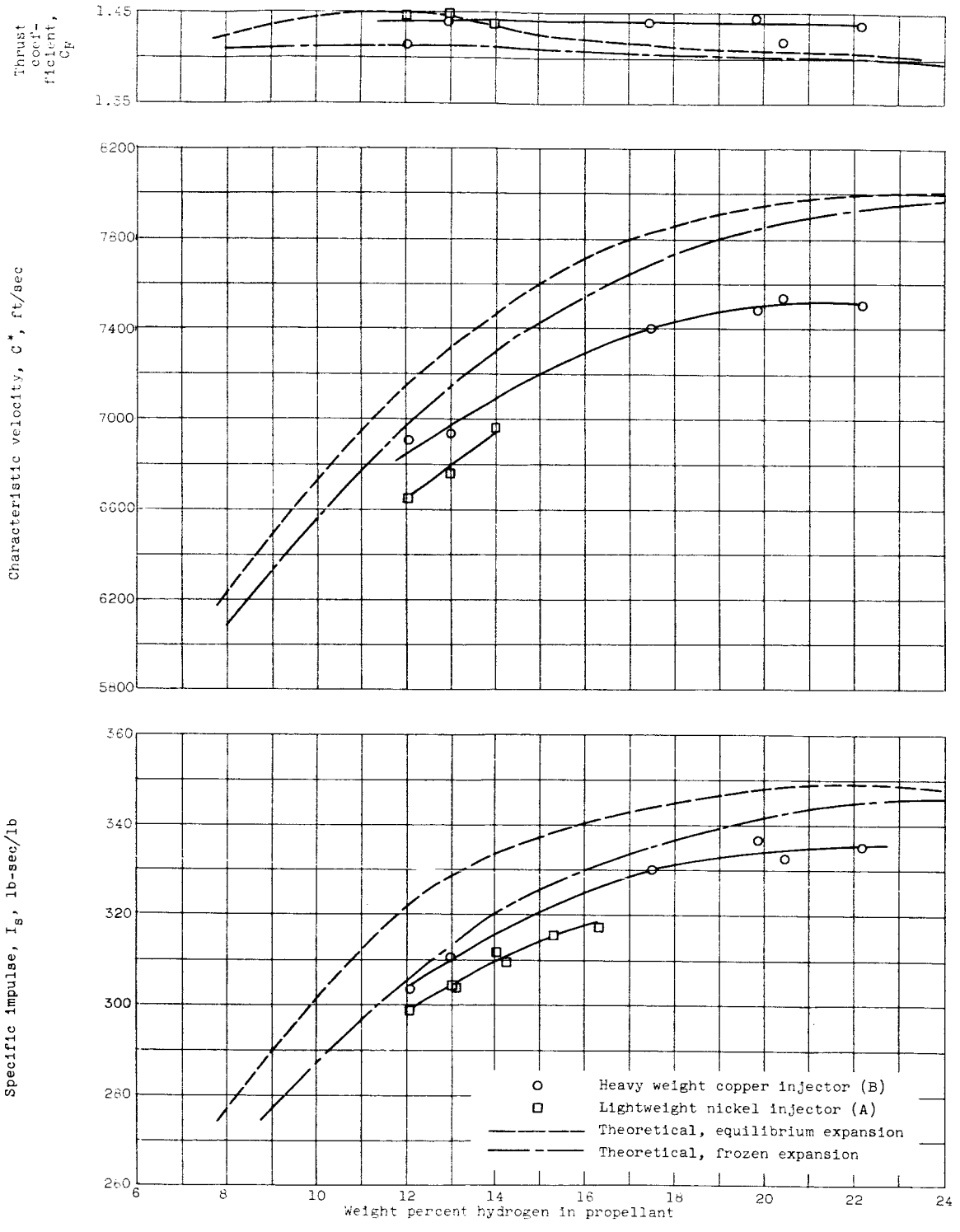

(a) Chamber pressure, 300 lb/sq in. abs; nominal thrust, 20,000 pounds; exhaust to ambient pressure, 14.4 lb/sq in. abs.

Figure 7. - Theoretical and experimental performance of hydrogen and oxygen in regeneratively cooled rocket engines. Expansion area ratio, 3.68.

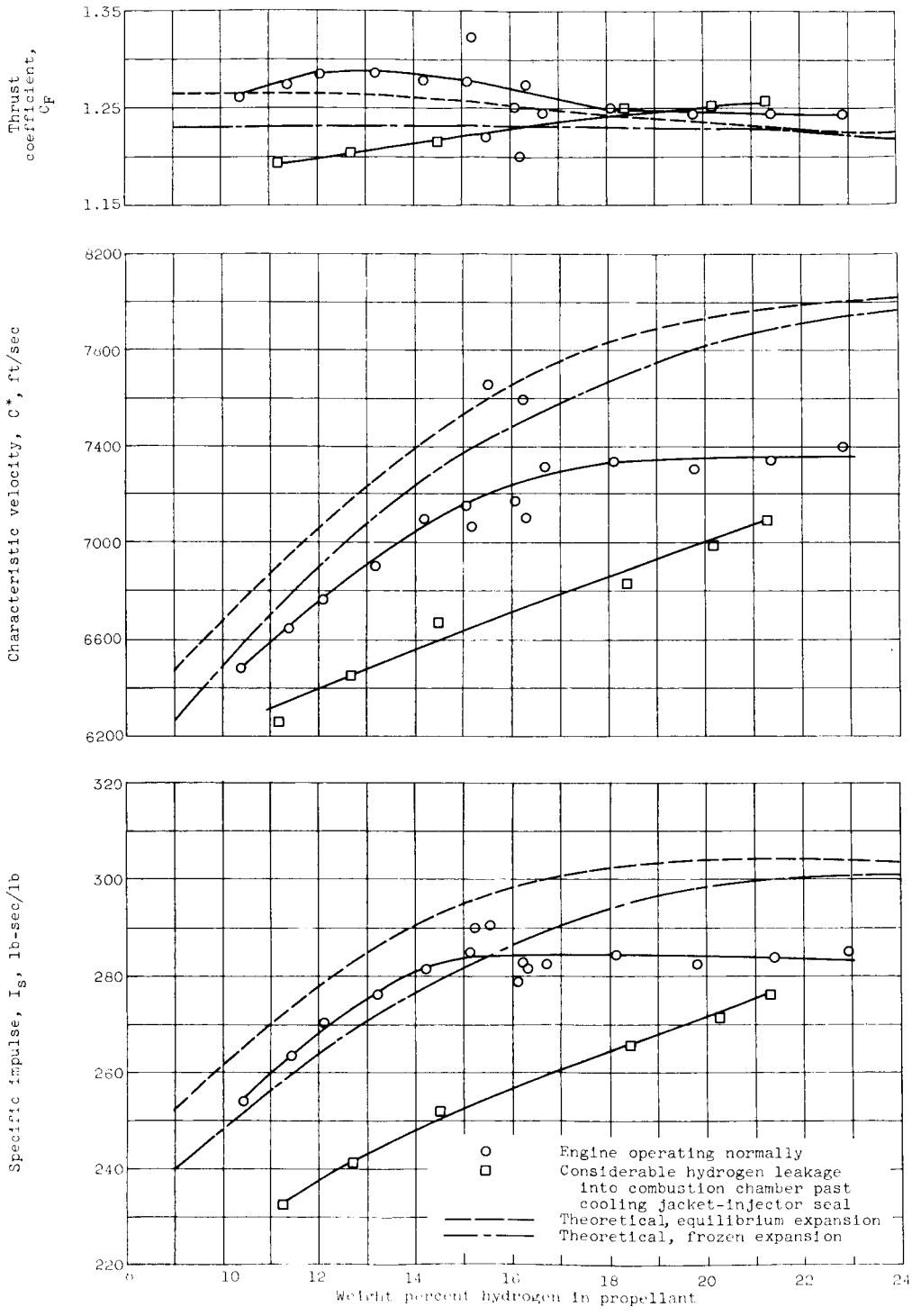

(b) Chamber pressure, 150 lb/sq in. abs; nominal thrust, 9100 pounds; exhaust to ambient pressure, 14.4 lb/sq in. abs; exhaust overexpanded at this pressure, no separation assumed; injectors A and A modified.

Figure 7. - Continued. Theoretical and experimental performance of hydrogen and oxygen in regeneratively cooled rocket engine. Expansion area ratio, 3.68.

[redacted]

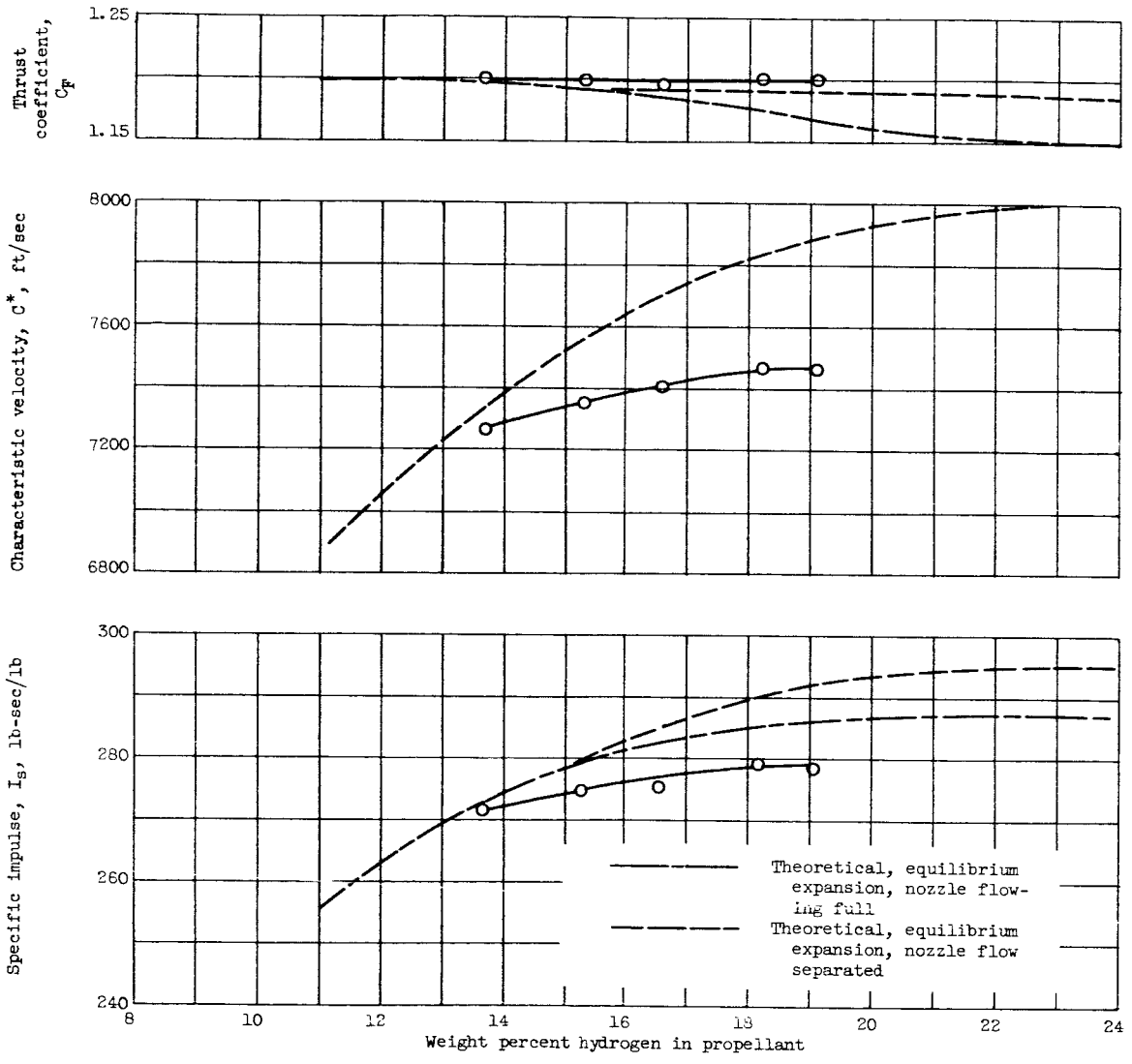

(c) Chamber pressure, 125 lb/sq in. abs; nominal thrust, 7200 pounds; exhaust to ambient pressure, 14.4 lb/sq in. abs; exhaust overexpanded at this pressure, separation assumed over part of range; injector A.

Figure 7. - Continued. Theoretical and experimental performance of hydrogen and oxygen in regeneratively cooled rocket engine. Expansion area ratio, 3.68.

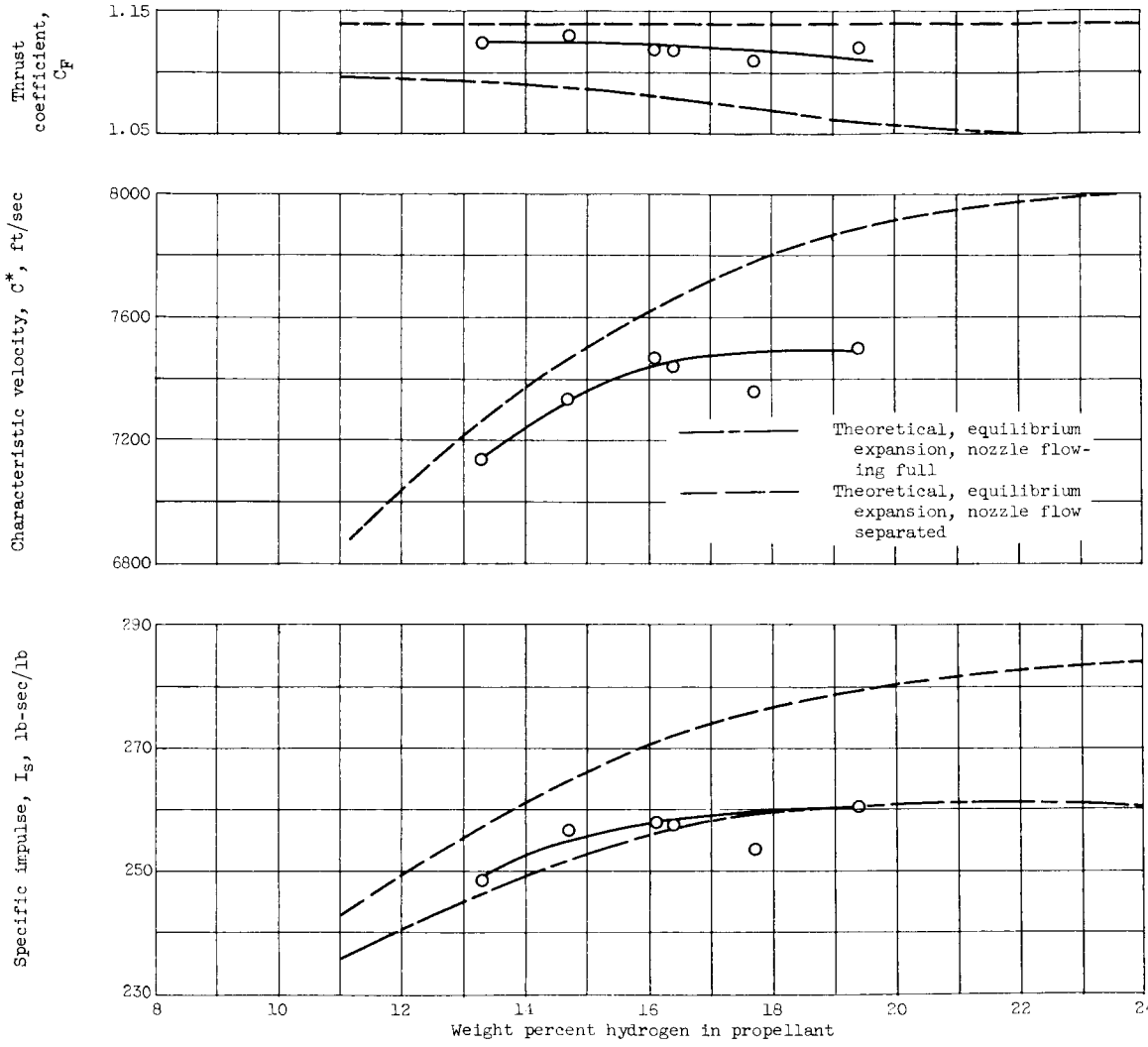

(d) Chamber pressure, 100 lb/sq in. abs; nominal thrust, 5300 pounds; exhaust to ambient pressure, 14.4 lb/sq in. abs; exhaust overexpanded at this pressure; separation assumed over whole range; injector A.

Figure 7. - Concluded. Theoretical and experimental performance of hydrogen and oxygen in regeneratively cooled rocket engine. Expansion area ratio, 3.68.

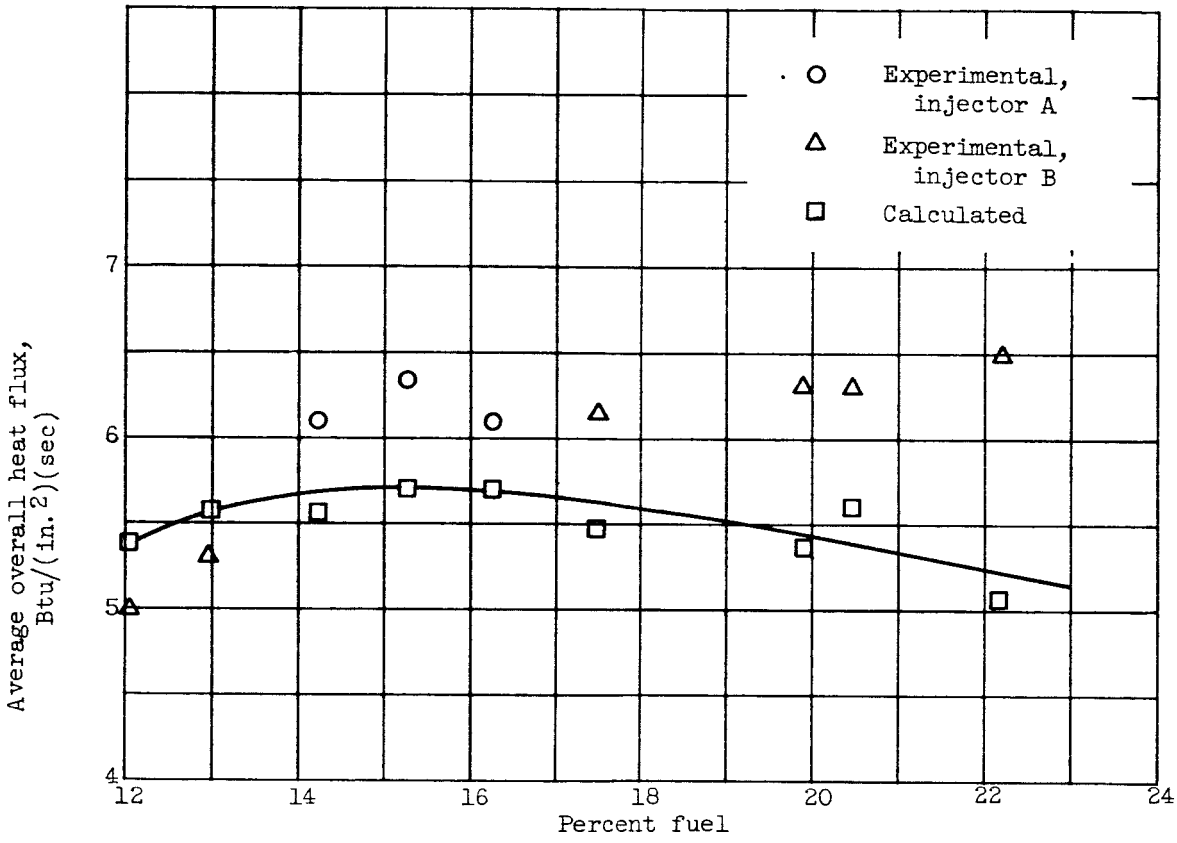

(a) Chamber pressure, 300 lb/sq in. abs.

Figure 8. - Heat-flux data. Contraction ratio, 1.9; expansion ratio, 3.68; expansion to 14.4 lb/sq in. abs.

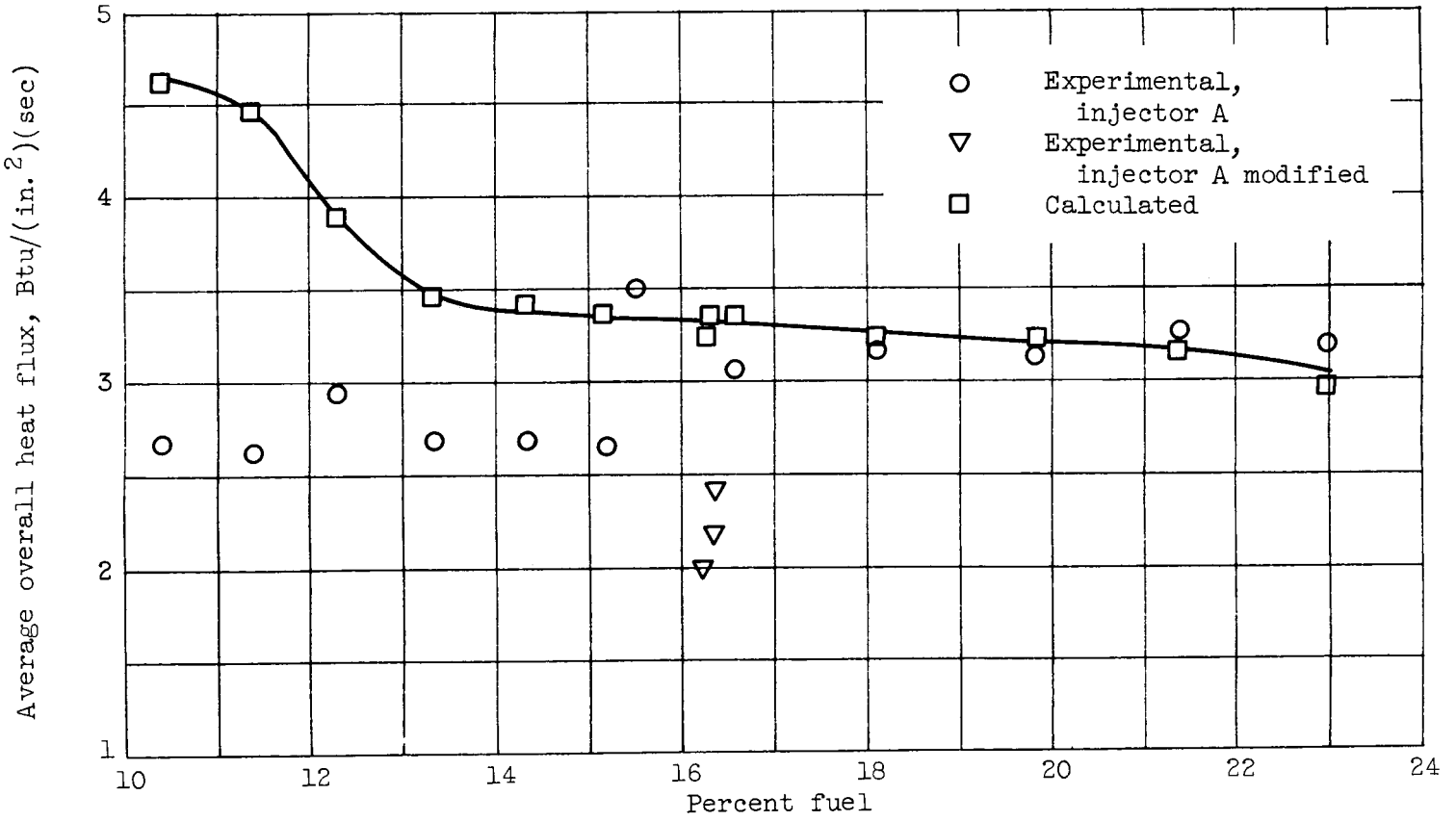

(b) Chamber pressure, 150 lb/sq in. abs.

Figure 8. - Continued. Heat-flux data. Contraction ratio, 1.9; expansion ratio, 3.68; expansion to 14.4 lb/sq in. abs.

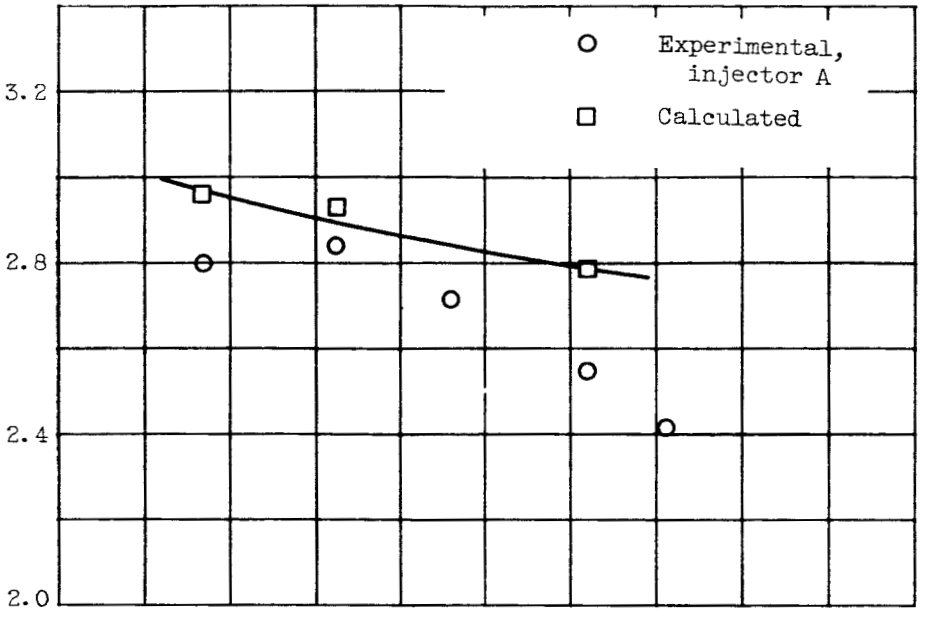

(c) Chamber pressure, 125 lb/sq in. abs.

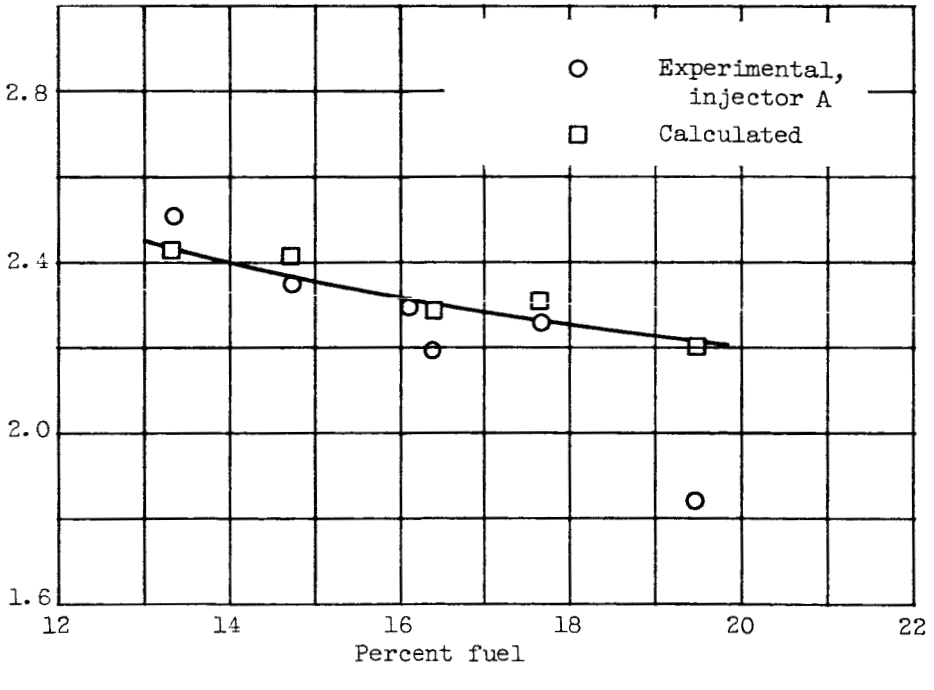

Average overall heat flux, Btu/(sec)(in.2)

(d) Chamber pressure, 100 lb/sq in. abs.

Figure 8. - Concluded. Heat-flux data. Contraction ratio, 1.9; expansion ratio, 3.68; expansion to 14.4 lb/sq in. abs.

Figure 9. - Typical hydrogen temperature distribution at cooling-jacket outlet showing orientation with respect to injector (A) face plate. Chamber pressure, 150 lb/sq in. abs; mixture ratios, 11.3 and 15.2 percent hydrogen; inlet temperature, 51° R.

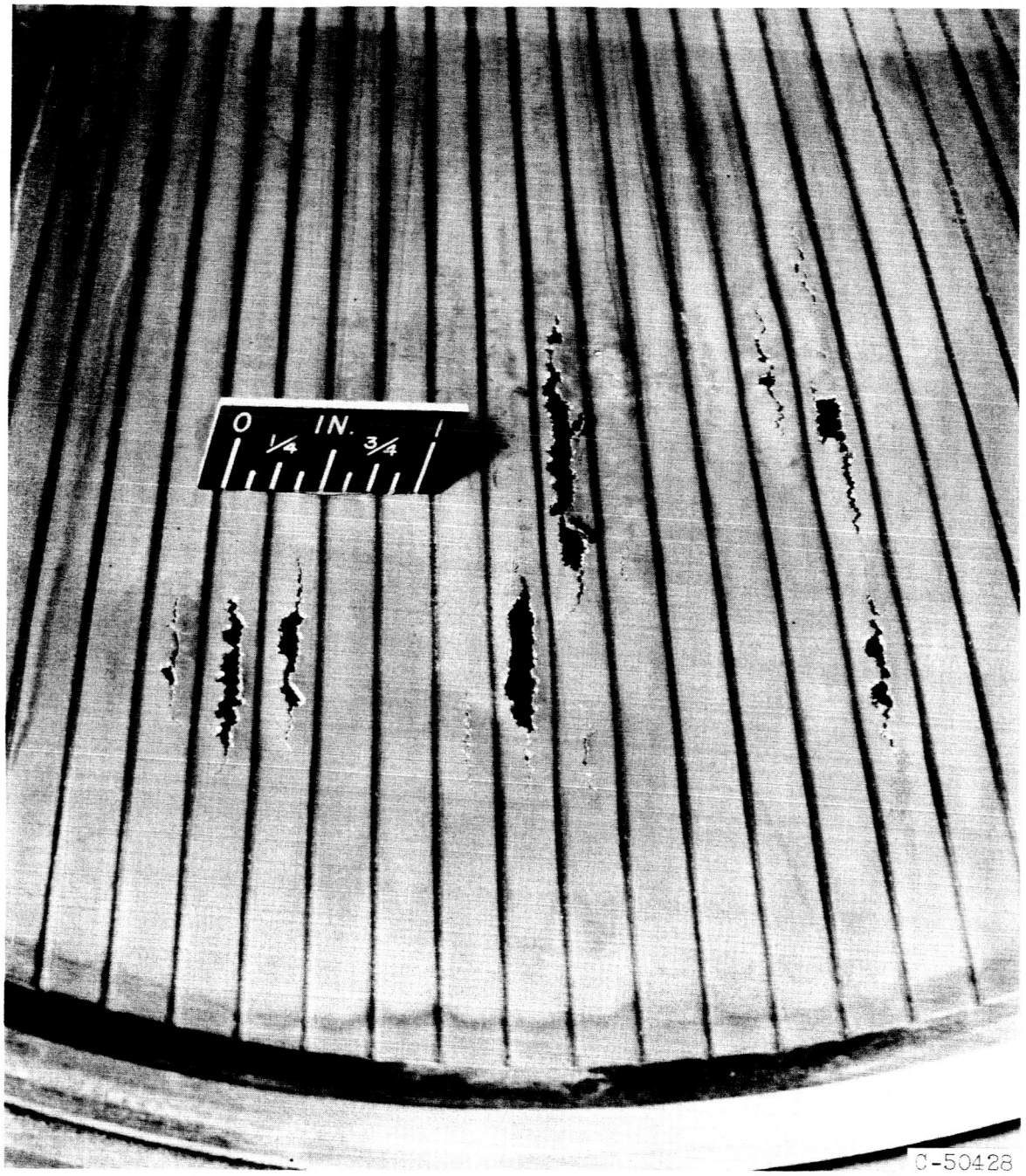

Figure 10. - Typical nickel-channel failures in combustion chamber after series of runs at chamber pressure of 300 lb/sq in. abs with mixture ratios from 12 to 14 percent fuel.

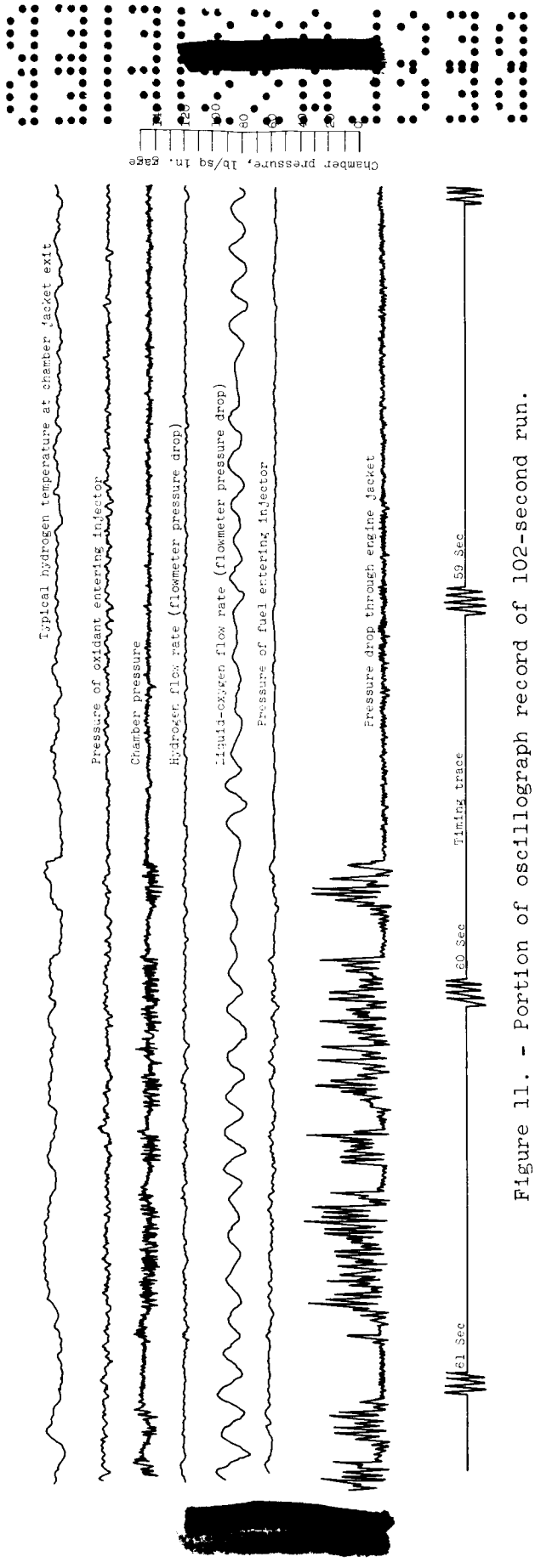

Figure 11. - Portion of oscillograph record of 102-second run.